PHOTONICS Research

Enhanced performance of a fast GaAs-based terahertz modulator via surface passivation

Yulian He,[1] Yuansheng Wang,[1] Qinghui Yang,[1] Huaiwu Zhang,[1] and Qiye Wen[1,2,*]

[1]School of Electronic Science and Engineering, State Key Laboratory of Electronic Thin Film and Integrated Devices, University of Electronic Science and Technology of China, Chengdu 610054, China
[2]Yangtze Delta Region Institute (Huzhou), University of Electronic Science and Technology of China, Huzhou 313001, China
*Corresponding author: qywen@uestc.edu.cn

Received 19 July 2021; revised 31 August 2021; accepted 5 September 2021; posted 9 September 2021 (Doc. ID 438196); published 21 October 2021

Surface-modified semiconductors show enormous potential for opto-terahertz (THz) spatial modulation due to their enhanced modulation depth (MD) along with their inherent broad bandwidth. Taking full advantage of the surface modification, a performance-enhanced, all-optical, fast switchable THz modulator was achieved here based on the surface-passivated GaAs wafer. With a decreased surface recombination rate and prolonged carrier lifetime induced by passivation, S-passivated GaAs was demonstrated as a viable candidate to enhance THz modulation performance in MD, especially at low photodoping levels. Despite a degraded modulation rate owing to the longer carrier lifetime, this passivated GaAs modulator simultaneously realizes a fast modulation at a 69-MHz speed and as high an MD as ∼94% in a spectral wideband of 0.2–1.2 THz. The results demonstrated a new strategy to alleviate the tradeoff between high MD and speed in contrast to bare surfaces or heterogeneous films/unusual geometry on semiconductors including Si, Ge, and GaAs. © 2021 Chinese Laser Press

https://doi.org/10.1364/PRJ.438196

1. INTRODUCTION

Recently, a growing research emphasis has been placed on terahertz (THz) radiation in view of its unique properties and potential applications in spectroscopy, noninvasive testing, and high-speed communications [1–3]. Being an imperative component in actual THz systems, considerable progress has been achieved in active modulators. These modulators are capable of complete adaptive manipulation of THz waves, primarily via electric, optical, or thermal stimuli. Among these, quasi-optical manipulation that allows fast transfer of information from the optical to THz regime is of particular interest [4]. A simple, but remarkable, opto-THz modulator is based on semiconductors, such as silicon (Si), germanium (Ge), or gallium arsenide (GaAs). When the semiconductor is irradiated by a laser with the photo energy larger than its bandgap, free carriers will be generated. These generated carriers form a temporary thin conductive layer at the surface. THz waves collimated onto this region are thus attenuated due to the increased reflection and absorption [5]. This kind of device realized by varying photocarrier populations predicts a broadband and cost-effective modulation method. Although such Si-based THz modulators are well established and significant advancement has been realized by cooperating with various heterogeneous films [6–9] and nanostructuring/microstructuring [10,11], they are mainly concentrated on photomodulation efficiency. Merely investigations on the response speed were reported. Because the carrier lifetime of Si is relatively long, typically $\tau_{\mathrm{eff}} \sim 100$ μs, the resultant modulation rate from these devices is limited to the order of ∼100 kHz [5]. With regard to Ge, even though it has higher mobility, which is beneficial for fast response, the representative value of τ_{eff} is tenfold longer compared to Si [5]. As a result, only a moderate speed of ∼200 kHz was realized [12,13]. Therefore, novel materials and approaches are sought for fast THz modulation.

An alternative highly investigated semiconductor for THz modulation is GaAs. GaAs has a direct bandgap of 1.44 eV, higher electron mobility than both Si and Ge, and a rather shorter carrier lifetime, on the order of picoseconds [14]. This makes GaAs an excellent candidate to realize fast THz modulation. However, there exists a trade-off between the modulation depth (MD) and speed because the MD depends on the accumulation of carriers, where a longer τ_{eff} indicates more carriers can be accumulated and thus a larger MD. On the contrary, fast speed requires a carrier lifetime τ_{eff} as short as possible. Therefore, such a smaller τ_{eff} in GaAs results in a limited MD of 13% [15]. To boost the modulation efficiency, unusual geometry, including photonic crystals [16] and gratings [17], has been coupled with GaAs to enhance the light–matter interaction. However, the enhancement is middling. They achieved a moderate MD level, far lower than the achievable value in its Si/Ge-based counterparts. Furthermore, this

additional resonant geometry not only introduces difficulty and complexity in the fabrication and the expenditure, but also limits the accessibility of these devices with a narrow frequency band. More importantly, all of these designs did not focus on the limiting factor itself, the short τ_{eff}. Recently, we found that surface passivation could effectively decrease surface recombination of photo-induced carriers in Si, lengthen the carrier lifetime, and thereby significantly enhance the MD of THz modulation [18]. This kind of improvement was further demonstrated by Hooper *et al.* [19] and our latest work [20]. As a result, it is taken for granted that such pretreatment will also be beneficial for MD improvement in GaAs-based devices, thus getting rid of its weakness in modulation efficiency.

As a proof of concept, here we designed and fabricated such a performance-enhanced modulator by passivating a GaAs surface with $(NH_4)_2S$. With passivation, a 5.6 times enhancement in the photoluminescence (PL) intensity and a 1.5 times longer carrier lifetime were achieved, which render S-passivated GaAs superior to bare GaAs in MD. This is especially true at low photodoping like 3 mW, where MD from the passivated one increased by 1.6 times compared to its bare GaAs counterpart. Moreover, the larger the pumping power, the higher the resultant MD. When it was increased to 60 mW, a comparable MD of 94% to that in a Si/Ge-based one at equivalent photodoping was received, along with a fast response rate of 69 MHz. Even though the rate was slightly degraded due to the longer carrier lifetime after passivation, it is still much faster than the 100 kHz magnitude by Si/Ge-based THz modulators. Hence, a fast, all-optical spatial THz modulation in a spectral broadband ranging from 0.2 THz to 1.2 THz is demonstrated by surface-passivating GaAs wafers. This kind of performance-enhanced, fast modulator is highly desirable in actual situations and offers a viable avenue to equilibrating the compromise between MD and speed.

2. MATERIAL PREPARATION AND CHARACTERIZATION

The investigations were performed on the semi-insulating n-GaAs(100) wafers, with a thickness of 625 μm and dark resistivity $>10^8\ \Omega\cdot$cm. Even though the low-temperature-grown GaAs has been a commercial substrate and shows an excellent performance in THz antenna, however, its typical τ_{eff} is only a few picoseconds or even subpicoseconds [21,22]. Thus, with regard to THz modulation, such a low τ_{eff} will only lead to a worsening modulation performance rather than enhancing the performance; in other words, low-temperature-grown GaAs is not a suitable candidate in such opto-THz modulators. Therefore, in this paper the semi-insulating GaAs with τ_{eff} of several hundred picoseconds was selected for our investigation. These semi-insulating GaAs wafers were pre-treated with acetone, absolute ethanol, and deionized water for 5 min to degrease and remove the impurities. Some of the samples after pretreatment were adopted as the reference set, bare GaAs. The rest were prepared for sulfidizing with the following procedure. They were first etched in a $1{:}5H_2SO_4{:}H_2O$ acid solution for 1 min for the removal of native oxides, and immediately surface-passivated by being immersed in a saturated solution of ammonium sulfide $[(NH_4)_2S]$ and tert-butanol (C_4H_9OH) for 20 min at a temperature of 50°C. Thus, a desirable S-passivated GaAs was fabricated.

The optical absorption was measured by an ultraviolet/visible/infrared (UV/VIS/IR) spectroscopy (PerkinElmer Lambda 750), and the PL intensity of GaAs samples under investigation was measured by a steady-state and transient fluorescence spectrometer (Edinburgh Instruments, FLS980). By means of a homemade optically pumped terahertz-probe (OPTP) spectroscopy system, the carrier lifetime of GaAs samples was determined. The THz time-domain signals transmitted through both GaAs samples were also detected by this OPTP system. For the dynamic modulation of a continuous THz wave (~340 GHz), a Schottky diode was assembled to record the THz intensity in dependence on time.

3. RESULTS AND DISCUSSION

As a measure of passivation efficiency, the PL properties in both GaAs wafers without and with surface treatment were investigated and considerably improved in the surface-passivated one. As shown in Fig. 1(a), the greatest increase of the PL intensity of S-passivated GaAs relative to bare GaAs achieves a 5.8-fold increase, which stems from the effective removal of oxides from the GaAs surface during the acid treatment and the following formation of sulfides by sulfur passivation. These courses lower the surface states and result in an attendant reduction of the surface recombination velocity [23], which indicates that a longer lifetime of surface carriers will be induced.

For the verification of the relation between PL intensity and carrier lifetime, an all-optical alternative technique (OPTP), was adopted, which is also referred to as time-resolved THz spectroscopy. This OPTP system has been demonstrated to be able to characterize optical and electrical properties of semiconductors that circumvents the need for PL and electrical

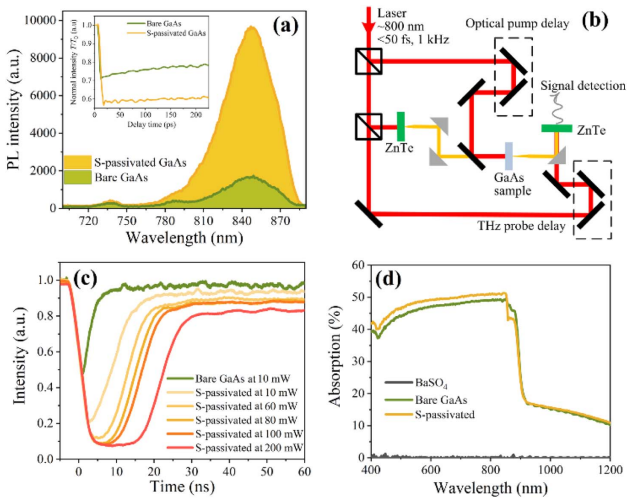

Fig. 1. Characterization of GaAs wafers before and after surface passivation. (a) PL spectra (inset: time-resolved THz transmission for the S-passivated GaAs and the reference bare GaAs measured at a low fluence of 3 mW); (b) schematic of the home-made OPTP setup; (c) response waveform of the bare and S-passivated GaAs based modulators to one pulse of the laser under different power levels; and (d) measured UV/VIS/IR absorption spectra.

contacts [24,25]. By means of this pump-and-probe scheme, an ultrashort optical pump arrives at the surface of the sample, creating a photo-carrier population that is probed by a THz pulse. By monitoring the transmission at a fixed probe position, and time-resolving the pump, the carrier lifetime can be estimated [26]. We homemade such an OPTP spectroscopy system and the setup is shown in Fig. 1(b). A femtosecond pulse laser centered at 800 nm with duration of <50 fs and a repetition rate of 1 kHz is undertaken. The pulses are split into the optical pump beam, THz generation beam, and detection beam. Both the optical pump and THz probe beams are equipped with a delay stage with attempts to control the optical pump timing on the surface of GaAs sample and the detection time, respectively. They are also redirected so that they can be collinearly and normally incident to the GaAs sample. When measuring the carrier lifetime, the THz probe delay stage was fixed at the peak of the THz pulse during the measurement procedure. The arrival of the pump beam at the GaAs surface generates photo-carriers that are available to absorb the THz probe and disappear over time due to trapping or recombination. The photo-carrier population was monitored by recording the transmitted THz amplitude from a time before the pumping arrives until a sufficient duration later. The inset of Fig. 1(a) shows the measured time-resolved THz transmission for the S-passivated GaAs and the reference bare GaAs at a low fluence of 3 mW. By fitting with double exponential decay functions, the resultant lifetime of carriers is roughly estimated to ~900 ps for S-passivated GaAs and ~600 ps for the bare one. After passivation, the carrier lifetime was lengthened by 1.5 folds, which is well matched with the one reported in Ref. [27]. Both the enhanced PL intensity and lengthened carrier lifetime indicate that the GaAs surface was well passivated when dipping in the saturated solution of $(NH_4)_2S$ and C_4H_9OH.

This type of subnanosecond carrier lifetime indicates a fast response of THz modulation. With a 340 GHz carrier, the dynamic response waveforms, through the bare and S-passivated GaAs-based modulators, to one of the pulses of the pumping laser were detected. As exhibited in Fig. 1(c), the intensities via both bare and S-passivated GaAs samples decline quickly at an almost identical speed. Then a slower recovery process is observed in the S-passivated one because the photo-generated electron-hole pairs usually can be generated in a very short time upon photodoping. Its recovery, however, is dependent on the recombination time, owing to the longer one that is positively correlated with the carrier lifetime, hence resulting in a longer recovery time after passivation. Remember the definition of response time in Ref. [5]: the time taken to modulate THz beam from 90% to 10% intensity as transfer time and that taken to return from 10% to 90% as recovery time. The response time for bare and S-passivated GaAs under 10 mW excitation was estimated to be 6.575 ns and 12.5125 ns, respectively. Hence, response rates of 154 MHz and 80 MHz can be calculated, respectively. Despite this, the speed was approximately halved in the S-passivated GaAs-based modulator due to the lengthened carrier lifetime by surface-passivating; as high as 80 MHz speed is still rather tantalizing with regard to the ~100 kHz magnitude in Si/Ge-based modulators [12,13]. This result also supports the conclusion above that the GaAs surface was effectively passivated by sulfur, which prolongs the lifetime of the surface carriers. More importantly, the descent of the THz amplitude thru S-passivated GaAs is much larger than that going through bare GaAs, which hints at a higher photomodulation efficiency for the THz modulator composed of the S-passivated GaAs wafer.

We also measured the UV/VIS/IR absorption spectra of GaAs specimens without and with surface passivation. The results are plotted in Fig. 1(d) and obviously show that S-passivated GaAs has better laser absorption than the reference one from 400 nm to 854 nm. An increase of ~1.8% is observed at the 800 nm pumping laser. This predicts that ~1.8% more photo-carrier density should be generated in the S-passivated Si even without consideration of its prolonged carrier lifetime. The reason is that the carrier concentration ΔN generated by optical excitation is quantitated by the product of carrier lifetime τ_{eff} and the generation rate of electron-hole pairs g. For a given optical excitation, the only parameter of significance in determining g is the laser absorption. The g value is proportionate to the absorption and their detailed correlation is formulated in Eq. (1) from now on. These three observations (higher PL intensity, longer carrier lifetime, and larger laser absorption) above all render the S-passivated GaAs an optimal candidate to perform a better THz modulation.

To elucidate the surface-passivation influence on this kind of GaAs-based opto-THz modulator, the THz modulation properties of GaAs wafers before and after passivating were investigated by the OPTP spectroscopy. The prototype and spatial configuration of the S-passivated GaAs-based THz modulator are shown in Fig. 2(a), where the 800 nm optical pump pulse has a spot diameter of 5 mm to completely encapsulate the incident THz beam (3 mm). The transmitted

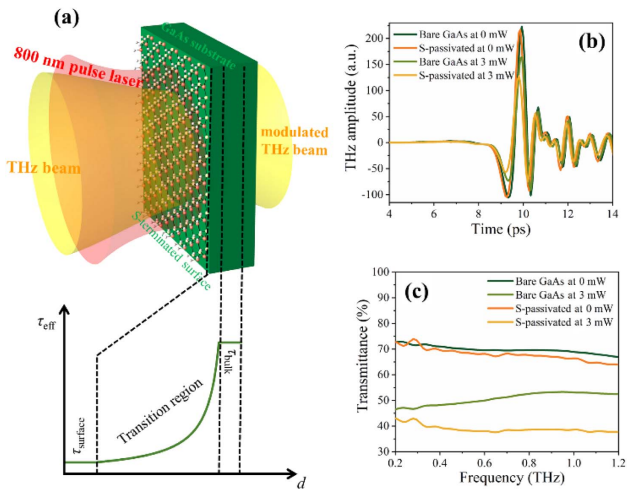

Fig. 2. Characterization of THz modulation performance through the S-passivated and bare GaAs samples. (a) Schematic of the S-passivated GaAs based all-optical spatial THz modulator, where an 800 nm pulse laser is adopted as optical excitation, which has a spot diameter of 5 mm to completely encapsulate the incident THz beam (3 mm). Bottom graph illustrates the penetration depth (d) dependence of the effective carrier lifetime (τ_{eff}) when the photodoping power is varied. (b) Detected transmitted time domain spectra; and (c) corresponding frequency domain spectra calculated from (b).

THz signals through the bare and S-passivated GaAs samples with and without a pumping laser are presented in Fig. 2(b). Under no photodoping, an infinitesimal reduction of 2.2% in the peak-to-peak amplitude of the main pulse was observed for the surface-passivated one. This results from the slightly increased charge density at the surface, which is induced by the decreased surface recombination velocity [19,20]. Upon pumping at a laser fluence of 3 mW, both bare and S-passivated GaAs wafers show considerable degradations in the amplitudes of transmitted THz waves, resulting from the increased reflection/absorption of the conductive layer formed by photogenerated electron-hole pairs at the samples' surfaces [12]. By Fourier transforming the time-domain spectra in Fig. 2(b) and normalizing to a reference spectrum measured in air, the corresponding transmission spectra in the frequency domain are plotted in Fig. 2(c). The increased conductivity contributes to the transmission attenuation over a wide frequency range from 0.2 THz to 1.2 THz, indicating a broadband modulation performance in THz regime. Obviously, this attenuation is more remarkable for the passivated sample. When no photodoping is applied, the averaged transmittance (T_{ave}) over the frequency window of 0.2–1.2 THz is 69.8% and 68.0% through bare and S-passivated GaAs, respectively. It declines to 50.9% for bare GaAs, but is much lower for the S-passivated one (38.9%) under 3 mW pumping. By defining the modulation depth $\mathrm{MD} = |T_{\mathrm{ave},x} - T_{\mathrm{ave},0}|/T_{\mathrm{ave},0}$ to be the difference between the averaged transmittance $T_{\mathrm{ave},0}$ without photodoping and that under x illumination normalized to $T_{\mathrm{ave},0}$, the calculated MD corresponds to 27.4% and 42.7%. As expected, an ~1.6-fold MD enhancement is experimentally realized by passivating the GaAs surface with sulfur.

More detailed experiments reveal that the S-passivated GaAs-based modulator is better when compared to the bare GaAs one with respect to the obtainable MD, especially at low photodoping levels. Figures 3(a) and 3(c) plot the transmitted THz domain signals under different photodoping levels for bare and S-passivated GaAs samples, respectively, with the corresponding frequency-domain spectra shown in Figs. 3(b) and 3(d). Obviously, both modulators present considerable and broadband attenuation in THz transmission under illumination, resulting from photo-induced electron-hole pairs. It is worth noting that, compared to bare GaAs, the transmission decay in S-passivated GaAs is more remarkable under equivalent power, especially at low power levels. For visualized observation, we summarized the averaged transmittance dependence on the photodoping power P and the resultant curves are shown in Fig. 3(e). At the low-power region, the transmittance through S-passivated GaAs is significantly lower than that through the bare one at an identical power level. The difference in T_{ave} reaches the maximum of $\Delta T_{\mathrm{ave}} = 11.7\%$ at $P = 3$ mW. Then, as the power level increases, photodoping tends to saturate, and the transmission deviation is increasingly lessened. The transmittance starts converging to a comparable value when P exceeds 10 mW. This behavior is also mirrored by MD, which is displayed in Fig. 3(f) as a function of P. Similar to the observation of the THz transmission variation in Fig. 3(e), a maximum enhancement of MD was observed at the low-power region up to 3 mW. Its ability to further increase the power deteriorates due to the saturation effect. Although the achieved MD in the two samples are comparable when $P > 10$ mW, the modulation by S-passivated GaAs is always superior under equivalent power photodoping. At 60 mW photodoping, an MD as high as 93.9% was obtained, which is comparable to that reported in its Si-based counterpart at an equivalent power level of photodoping [28].

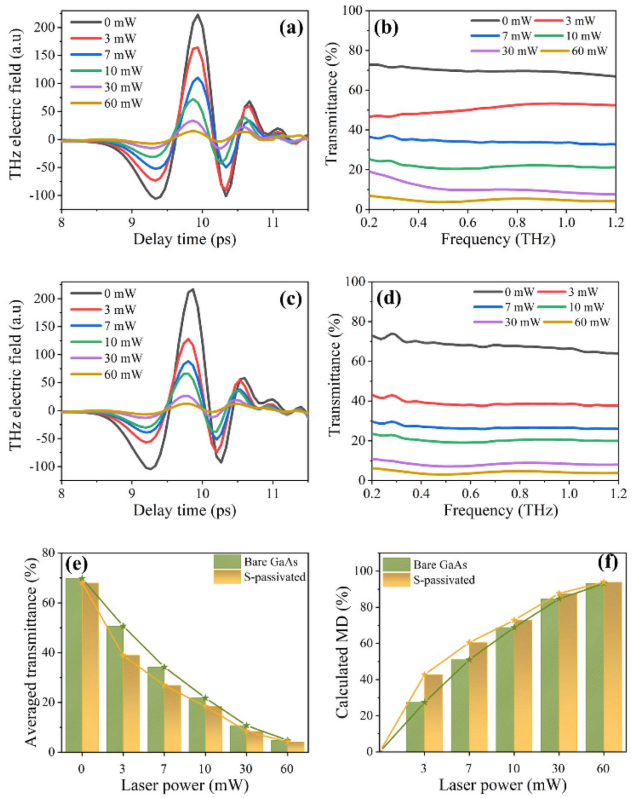

Fig. 3. THz modulation performance under 800 nm femtosecond laser with different power: (a) and (c) time-domain spectra; (b) and (d) corresponding frequency-domain spectra for bare and S-passivated GaAs, respectively. (e) THz averaged transmittance over a frequency window from 0.2 THz to 1.2 THz; and (f) calculated MD in dependence on the pumping laser power as measured for bare GaAs and S-passivated GaAs wafers.

The varying manners of transmission and MD relative to laser power can be qualitatively elucidated by the generation and recombination processes of electron-hole pairs in GaAs under photodoping. When an optical excitation is applied whose photo energy exceeds the bandgap of GaAs, electron-hole pairs (carriers) are generated in the substrate and the residual carrier population in the GaAs wafer can be evaluated by

$$(\Delta N)_0 = g\tau_{\mathrm{eff}} = \frac{aP}{d\hbar\nu}\tau_{\mathrm{eff}}. \tag{1}$$

Here, g is the generation rate of electron-hole pairs and is determined by the power of incident laser P, the portion of the incident photons that enter the wafer a [i.e., the laser absorption shown in Fig. 1(c), which is given by the laser transmission t and determined by the standard Fresnel equation], the depth that the photons penetrate into the wafer d, and the energy ($\hbar\nu$)

of the incident photons at frequency ν [19]. Therefore, the stronger illumination results in more photo-generated electron-hole pairs. These carriers contribute to an increase in the dielectric constant of GaAs specimens and a larger decrease in the transmittance of THz radiation according to the Drude model [29]. Hence, THz transmissions going through both bare and S-passivated GaAs wafers decrease as the power increases, as shown in Fig. 3(e), accompanied by an increased MD, as shown in Fig. 3(f).

The effective carrier lifetime τ_{eff} is determined by the carrier recombination process, including surface recombination and bulk recombination:

$$\frac{1}{\tau_{\text{eff}}} = \frac{1}{\tau_{\text{surface}}} + \frac{1}{\tau_{\text{bulk}}}, \tag{2}$$

where τ_{surface} is related to surface recombination that occurs due to the existence of defect states at the GaAs surfaces; τ_{bulk} is dependent on the quality of the GaAs wafer used. For a low photodoping level, the carriers were photo-generated in the vicinity of the GaAs surface and τ_{surface} can be approximately considered as τ_{eff} at this moment. Owing to the existence of native Ga/As oxides and dangling bonds, τ_{surface} is quite short for bare GaAs. For S-passivated GaAs, however, the treatment in the solution of $(NH_4)_2S$ and C_4H_9OH leads to an effective removal of oxides from its surface and to the formation of sulfides there, which efficiently prolongs τ_{surface}. At a low influence of 3 mW, for example, we previously measured τ_{eff} of ~600 ps and ~900 ps for bare and S-passivated GaAs, respectively, rendering a significant enhancement of MD in the S-passivated one. However, as the photodoping power increased, more carriers were produced and gradually diffused into the substrate, and τ_{eff} is then synergistically dominated by τ_{surface} and τ_{bulk}. With a concomitant effect, τ_{bulk} plays a progressively major role in the determination of τ_{eff} with growing power. Because these two GaAs wafers were selected from the same batch production, they generally have an identical τ_{bulk}, typically on the order of ~10 ns [5]. Thus, the higher the power, the smaller the deviation between the two resultant τ_{eff}. This implies a deteriorated enhancement of MD as shown in Fig. 3(f), so that the value of S-passivated GaAs approaches that of the bare one and reaches a comparative value at 60 mW due to the saturation effect.

This conclusion also can be supported by the dynamic modulation shown in Fig. 1(c), where the amplitudes of response waveforms remain steady when the power exceeds 60 mW and indicates that a fast modulation response of 69 MHz can be calculated. On the basis of an opto-THz modulation mechanism based on semiconductors, incident THz waves are attenuated due to the increased reflection/absorption formed by the photo-induced carriers. At a low photodoping, the generated carrier density is relatively low and the THz attenuation primarily originates from the absorption. The higher the photodoping, the more the carriers; the larger the absorption, the lower the transmission. Such an attenuation is saturated at 60 mW. When further increasing the power, the THz radiation is synergistically decreased by the absorption and reflection. Despite no further decline in the THz transmission, these superfluous photo-generated carriers make GaAs gradually metallic, which results in a flat signal. The higher the power, the more superfluous carriers that are generated, and the longer the flat duration. Such a flat signal reaches a maximum at an extreme photodoping level of 200 mW. As shown in Fig. 1(c), this flat signal begins at ~4.3 ns and ends at ~15.1 ns, defining a duration of ~10.8 ns, which is exactly a typical τ_{bulk} value of GaAs [5,27]. This result demonstrates that this signal indeed comes from the sample. It should be pointed out that such a high power was investigated with an attempt to further certify our preceding elucidation. To eliminate the saturation effects caused by the response limits of the equipment, in this paper we only pay attention to its modulation performance before saturating; that is, the photodoping range of 0–60 mW.

We also analyzed the changes in the photo-excited carrier density and photoconductivity with changes in the photodoping power by OPTP spectroscopy to thoroughly explain the photo-induced modulation mechanism for the transmitted THz waves. By taking the Fourier transform of the measured THz time-domain waveforms from the excited ($\tilde{E}_{\text{excited}}$) and unexcited ($\tilde{E}_{\text{unexcited}}$) sample at a specific pump time delay, the frequency-dependent transmission can be calculated by [26,30,31]

$$\tilde{T}(\omega) = \frac{\tilde{E}_{\text{excited}}(\omega)}{\tilde{E}_{\text{unexcited}}(\omega)} = \frac{n+1}{n+1+Z_0 d\tilde{\sigma}(\omega)}, \tag{3}$$

where $n = 3.48$ is the refractive index of unexcited GaAs in the THz region, $Z_0 = 377\ \Omega$ is the impedance of free space, and d is the thickness of the photo-excited layer, which is estimated to be 1 μm based on the penetration depth of the 800 nm pump in GaAs [31]. Thus, the complex conductivity $\tilde{\sigma}(\omega) = \sigma_{\text{re}}(\omega) + i\sigma_{\text{im}}(\omega)$ can be obtained from Eq. (3). Figure 4 shows the real part $[\sigma_{\text{re}}(\omega)]$ and the imaginary part $[\sigma_{\text{im}}(\omega)]$ of the calculated photoconductivity, respectively, from S-passivated and bare GaAs under various photodoping powers. Since the THz signal is greatly attenuated by the modulators, the calculation results in the higher or lower frequency range are not reliable, so we only show data between 0.7 THz and 1.7 THz here [30]. We also did not adopt the THz waveform data with the highest MD because it would introduce excessive noise errors. The data corresponding to lower photodoping power increasing from 0 mW to 30 mW were applied.

On the basis of the resultant complex conductivity, the carrier concentration can be qualitatively analyzed using the simple Drude model, which can be calculated by

$$N = m\varepsilon_0\omega_p^2/e^2, \tag{4}$$

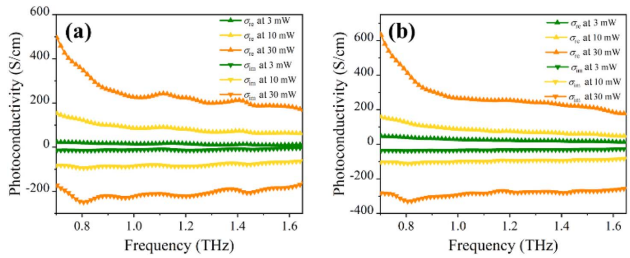

Fig. 4. Calculated complex conductivity from (a) bare and (b) S-passivated GaAs under various photodoping powers.

where m and e are the effective mass and charge of electron, respectively; ε_0 is the vacuum permittivity; and ω_p is the plasma frequency with an approximate expression as

$$\omega_p = \sqrt{\varepsilon_{\mathrm{im}}^2/(1-\varepsilon_{\mathrm{re}})}\omega. \tag{5}$$

Here, ω is the operational frequency; $\varepsilon_{\mathrm{re}}$ and $\varepsilon_{\mathrm{im}}$ are the real part and imaginary part of dielectric constant, respectively, and depend on the complex conductivity:

$$\varepsilon_{\mathrm{re}}(\omega) = 1 - \sigma_{\mathrm{im}}(\omega)/(\varepsilon_0\omega), \tag{6}$$

$$\varepsilon_{\mathrm{im}}(\omega) = \sigma_{\mathrm{re}}(\omega)/(\varepsilon_0\omega). \tag{7}$$

Thereafter, the photo-generated carrier density as a function of the photodoping power can be qualitatively drawn in Fig. 5. From Figs. 4 and 5, we can observe that both the real part of photoconductivity $\sigma_{\mathrm{re}}(\omega)$ and the carrier density N increase with an increase in the photodoping power. As we all know, $\sigma_{\mathrm{re}}(\omega)$ corresponds to the absorption coefficient, where a higher value means a higher absorption in THz radiation. A one-order increment of N also is achieved. This indicates that as the photodoping power increases, large numbers of electrons are induced, which are transferred and concentrate, thus significantly enhancing the electron–phonon scattering effect.

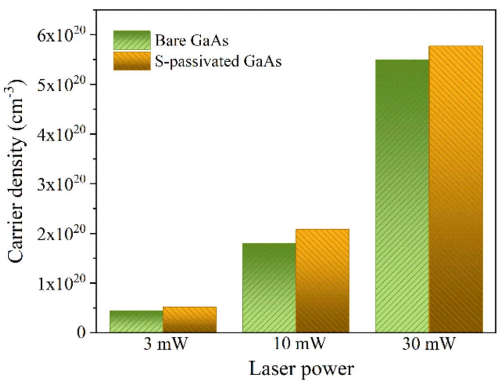

Fig. 5. Calculated carrier densities from bare and S-passivated GaAs as a function of photodoping power.

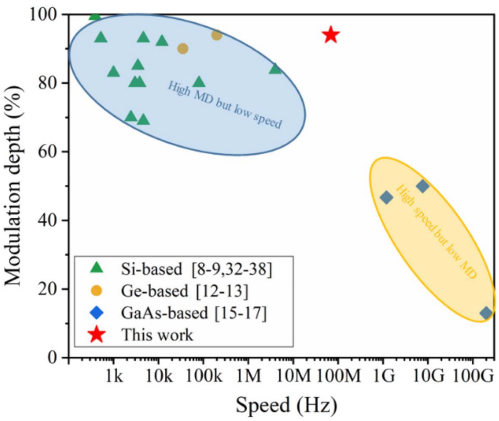

Fig. 6. Performance of opto-THz modulators based on different semiconductors.

Both larger $\sigma_{\mathrm{re}}(\omega)$ and N contribute to a lower transmission, as Fig. 3 shows.

To facilitate further comparison with other material systems, we collated representative results obtained from the state-of-the-art semiconductor-based opto-THz modulators [8,9,12,13,15–17,32–38], and present this summary in Fig. 6. The results show that both Si and Ge tend to produce high MD, but limited speed, while GaAs has fast modulation, but low MD. Despite various schemes adopted to enhance their modulation performance, a compromise still exists between MD related to the accumulation of carriers and speed depending on τ_{eff}. Our method balanced this compromise by prolonging τ_{eff} with surface-passivated GaAs and simultaneously realized as a high MD as ~94% and 69 MHz fast broadband THz modulation. Compared to these high-MD schemes, we believe our design exhibits a much faster modulation and a comparable modulation efficiency. With respect to these high-speed architectures, in spite of a deteriorated speed, our S-passivated GaAs-based modulator not only achieves a much higher MD but also a broadband modulation property.

4. CONCLUSION

In this paper, we demonstrated that surface passivation is an effective approach to improve modulation efficiency for GaAs-based photomodulators with only a small decrease in the response rate, especially at low photodoping levels. The influence of passivation on the fast carrier dynamics in GaAs and modulation performance of GaAs-based THz modulators was examined using OPTP spectroscopy. Increases of 5.8 times and 1.5 times, respectively, for the PL intensity and carrier lifetime were measured in a passivated GaAs wafer, which contributes to a spectrally wideband modulation of transmitted THz radiation in a frequency range from 0.2 THz to 1.2 THz, with a maximum averaged modulation depth up to ~94% at a proper excitation intensity. Such a high MD is comparable to these Si/Ge-based opto-THz modulators and is even far superior to the GaAs-based ones. The decreased modulation rate of this proposed modulator was measured as 69 MHz, which has yet to be reported in its Si/Ge-based counterparts. These results make our device an ideal candidate to eliminate the need for a trade-off between high MD and fast modulation speed. Such high-modulation performance and ease of fabrication also demonstrate the wide application possibilities for this device. As a result, we believe the proposed modulator has a promising future in THz imaging and communications technologies.

Funding. Science Challenge Project (TZ2018003); National Natural Science Foundation of China (61831012); International Science and Technology Cooperation Programme (2015DFR50870); Sichuan Province Science and Technology Support Program (2021JDTD0026).

Disclosures. The authors declare no conflicts of interest.

Data Availability. Data underlying the results presented in this paper are not publicly available at this time but may be obtained from the authors upon reasonable request.

REFERENCES

1. S. Zhong, "Progress in terahertz nondestructive testing: a review," Front. Mech. Eng. **14**, 273–281 (2019).
2. H. Aghasi, S. M. H. Naghavi, M. Tavakoli Taba, M. A. Aseeri, A. Cathelin, and E. Afshari, "Terahertz electronics: application of wave propagation and nonlinear processes," Appl. Phys. Rev. **7**, 021302 (2020).
3. Z. T. Ma, Z. X. Geng, Z. Y. Fan, J. Liu, and H. D. Chen, "Modulators for terahertz communication: the current state of the art," Research **2019**, 6482975 (2019).
4. M. Rahm, J.-S. Li, and W. J. Padilla, "THz wave modulators: a brief review on different modulation techniques," J. Infrared Millim. Terahertz Waves **34**, 1–27 (2013).
5. A. Kannegulla, M. I. B. Shams, L. Liu, and L.-J. Chen, "Photo-induced spatial modulation of THz waves: opportunities and limitations," Opt. Express **23**, 32098–32112 (2015).
6. S. Chen, F. Fan, Y. Miao, X. He, K. Zhang, and S. Chang, "Ultrasensitive terahertz modulation by silicon-grown MoS_2 nanosheets," Nanoscale **8**, 4713–4719 (2016).
7. W. Liu, F. Fan, S. Xu, M. Chen, X. Wang, and S. Chang, "Terahertz wave modulation enhanced by laser processed PVA film on Si substrate," Sci. Rep. **8**, 8304 (2018).
8. L.-Y. Xiong, B. Zhang, H.-Y. Ji, W. Wang, X. Liu, S.-L. He, and J.-L. Shen, "Active optically controlled broadband terahertz modulator based on Fe_3O_2 nanoparticles," IEEE Trans. Terahertz Sci. Technol. **8**, 535–540 (2018).
9. J.-P. Yu, S. Chen, F. Fan, S.-T. Xu, J.-R. Cheng, X.-F. Chen, L. Xiao, and S.-J. Chang, "Accelerating terahertz all-optical modulation by hot carriers effects of silver nanorods in PVA film," AIP Adv. **9**, 075017 (2019).
10. Z.-W. Shi, X.-X. Cao, Q.-Y. Wen, T.-L. Wen, Q.-H. Yang, Z. Chen, W.-S. Shi, and H.-W. Zhang, "Terahertz modulators based on silicon nanotip array," Adv. Opt. Mater. **6**, 1700620 (2018).
11. Q.-Y. Wen, Y.-L. He, Q.-H. Yang, P. Yu, Z. Feng, W. Tan, T.-L. Wen, Y.-X. Zhang, Z. Chen, and H.-W. Zhang, "High-performance photo-induced spatial terahertz modulator based on micropyramid silicon array," Adv. Mater. Technol. **5**, 1901058 (2020).
12. Q.-Y. Wen, W. Tian, Q. Mao, Z. Chen, W.-W. Liu, Q.-H. Yang, M. Sanderson, and H.-W. Zhang, "Graphene based all-optical spatial terahertz modulator," Sci. Rep. **4**, 7409 (2014).
13. Y. P. Li, D. N. Zhang, Y. L. Liao, Q. Y. Wen, Z. Y. Zhong, and T. L. Wen, "Interface engineered germanium for infrared THz modulation," Opt. Mater. **111**, 110659 (2021).
14. E. Herrmann, H. Gao, Z. X. Huang, S. R. Sitaram, K. Ma, and X. Wang, "Modulators for mid-infrared and terahertz light," J. Appl. Phys. **128**, 140903 (2020).
15. S. A. Baig, J. L. Boland, D. A. Damry, H. H. Tan, C. Jagadish, H. J. Joyce, and M. B. Johnston, "An ultrafast switchable terahertz polarization modulator based on III–V semiconductor nanowires," Nano Lett. **17**, 2603–2610 (2017).
16. L. Fekete, F. Kadlec, P. Kužel, and H. Němec, "Ultrafast opto-terahertz photonic crystal modulator," Opt. Lett. **32**, 680–682 (2007).
17. L. Y. Deng, J. H. Teng, H. W. Liu, Q. Y. Wu, J. Tang, X. H. Zhang, S. A. Maier, K. P. Lim, C. Y. Ngo, S. F. Yoon, and S. J. Chua, "Direct optical tuning of the terahertz plasmonic response of InSb subwavelength gratings," Adv. Opt. Mater. **1**, 128–132 (2013).
18. Q.-Y. Wen, H. Zhang, C.-Y. Shen, Y.-L. He, Q.-H. Yang, W. Tan, Z. Feng, and H.-W. Zhang, "Terahertz modulator based on silicon-based microstructure on SOI, system and method," CN Patent 201910376814.8 (7 May, 2019).
19. I. R. Hooper, N. E. Grant, L. E. Barr, S. M. Hornett, J. D. Murphy, and E. Hendry, "High efficiency photomodulators for millimeter wave and THz radiation," Sci. Rep. **9**, 18304 (2019).
20. Y.-L. He, Y.-S. Wang, M. Li, Q.-H. Yang, Z. Chen, J. Zhang, and Q.-Y. Wen, "All-optical spatial terahertz modulator with surface-textured and passivated silicon," Opt. Express **29**, 8914–8925 (2021).
21. V. K. Mag-usara, S. Funkner, G. Niehues, E. A. Prieto, M. H. Balgos, A. Somintac, E. Estacio, A. Salvador, K. Yamamoto, M. Hase, and M. Tani, "Low temperature-grown GaAs carrier lifetime evaluation by double optical pump terahertz time-domain emission spectroscopy," Opt. Express **24**, 26175–26185 (2016).
22. M. Tani, S. Matsuura, K. Sakai, and S. I. Nakashima, "Emission characteristics of photoconductive antennas based on low-temperature-grown GaAs and semi-insulating GaAs," Appl. Opt. **36**, 7853–7859 (1997).
23. V. N. Bessolov, E. V. Konenkova, and M. V. Lebedev, "Solvent effect on the properties of sulfur passivated GaAs," J. Vac. Sci. Technol. B **14**, 2761–2766 (1996).
24. M. C. Beard, G. M. Turner, and C. A. Schmuttenmaer, "Transient photoconductivity in GaAs as measured by time-resolved terahertz spectroscopy," Phys. Rev. B **62**, 15764–15777 (2000).
25. R. Ulbricht, "Carrier dynamics in semiconductors studied with time-resolved terahertz spectroscopy," Rev. Mod. Phys. **83**, 543–586 (2011).
26. J. Afalla, K. C. Gonzales, E. A. Prieto, G. Catindig, J. D. Vasquez, H. A. Husay, M. A. Tumanguil-Quitoras, J. Muldera, H. Kitahara, A. Somintac, A. Salvador, E. Estacio, and M. Tani, "Photoconductivity, carrier lifetime and mobility evaluation of GaAs films on Si (100) using optical pump terahertz probe measurements," Semicond. Sci. Technol. **34**, 035031 (2019).
27. J. Lloyd-Hughes, S. K. E. Merchant, L. Fu, H. H. Tan, C. Jagadish, E. Castro-Camus, and M. B. Johnston, "Influence of surface passivation on ultrafast carrier dynamics and terahertz generation in GaAs," Appl. Phys. Lett. **89**, 232102 (2006).
28. P. Weis, J. L. Garcia-Pomar, M. Hoh, B. Reinhard, A. Brodyanski, and M. Rahm, "Spectrally wide-band terahertz wave modulator based on optically tuned graphene," ACS Nano **6**, 9118–9124 (2012).
29. J. Mrozek and H. Nemec, "Calculation of terahertz conductivity spectra in semiconductors with nanoscale modulation," Phys. Rev. B **86**, 075308 (2012).
30. T. He, B. Zhang, G.-C. Wang, M.-D. Zang, T.-B. Hou, and J.-L. Shen, "High efficiency THz-wave modulators based on conjugated polymer-based organic films," J. Phys. D **49**, 075111 (2016).
31. Q.-L. Zhou, Y. Shi, B. Jin, and C. Zhang, "Ultrafast carrier dynamics and terahertz conductivity of photoexcited GaAs under electric field," Appl. Phys. Lett. **93**, 102103 (2008).
32. T.-L. Wen, D.-N. Zhang, Q.-Y. Wen, Y.-L. Liao, C. Zhang, J.-Y. Li, W. Tian, Y.-P. Li, H.-W. Zhang, Y.-X. Li, Q.-H. Yang, and Z.-Y. Zhong, "Enhanced optical modulation depth of terahertz waves by self-assembed monolayer of plasmonic gold nanoparticles," Adv. Opt. Mater. **4**, 1974–1980 (2016).
33. G.-C. Wang, B. Zhang, H.-Y. Ji, X. Liu, T. He, L.-F. Lv, Y.-B. Hou, and J.-L. Shen, "Monolayer graphene based organic optical terahertz modulator," Appl. Phys. Lett. **110**, 023301 (2017).
34. D.-D. Liu, W. Wang, L.-Y. Xiong, H.-Y. Ji, B. Zhang, and J.-L. Shen, "High-efficiency optical terahertz modulation of organometallic halide perovskite nanoplates on silicon," Opt. Mater. **96**, 109368 (2019).
35. Y.-P. Li, T.-L. Wen, D.-N. Zhang, H.-L. Lu, Y.-L. Liao, X.-H. Wang, H.-W. Zhang, and Z.-Y. Zhong, "Comparison study of gold nanorod and nanoparticle monolayer enhanced optical terahertz modulators," IEEE Trans. Terahertz Sci. Technol. **9**, 484–490 (2019).
36. Y.-P. Li, D.-N. Zhang, R.-T. Jia, X.-S. Li, Y.-L. Liao, Q.-Y. Wen, Z.-Y. Zhong, and T.-L. Wen, "Mechanism and optimization of a graphene/silicon hybrid diode terahertz modulator," ACS Appl. Electron. Mater. **2**, 1953–1959 (2020).
37. Q. Li, Z. Tian, X. Zhang, R. Singh, L. Du, J. Gu, J. Han, and W. Zhang, "Active graphene-silicon hybrid diode for terahertz waves," Nat. Commun. **6**, 7082 (2015).
38. J.-S. Li and M.-S. Hu, "Enhancement of silicon modulating properties in the THz range by YAG-Ce coating," Sci. Rep. **10**, 6605 (2020).